cosmetics

MDPI

Article

Enhanced Antimicrobial Activity of Silver Sulfadiazine Cosmetotherapeutic Nanolotion for Burn Infections

Qurat-ul ain Fatima [1], Naveed Ahmed [1,*], Bazla Siddiqui [1], Asim ur Rehman [1], Ihsan ul Haq [1], Gul Majid Khan [1,2] and Abdelhamid Elaissari [3]

[1] Department of Pharmacy, Quaid-i-Azam University, Islamabad 45320, Pakistan
[2] Islamia College University, Peshawar 25120, Pakistan
[3] CNRS, ISA-UMR 5280, Univ Lyon, University Claude Bernard Lyon-1, 69622 Villeurbanne, France
* Correspondence: natanoli@qau.edu.pk

Abstract: Burns are highly traumatizing injuries that can be complicated by various microbial infections, leading to morbidity and mortality. The ultimate goal of burn therapy is to prevent any microbial infection and rapid wound healing with epithelization. The current study aimed to develop and investigate the potential of nanoemulsion-based cosmetotherapeutic lotion of silver sulfadiazine (SSD) for increased antimicrobial activity to treat burn injuries. Silver sulfadiazine is the standard topical treatment for burn patients, but is allied with major limitations of poor solubility, low bioavailability, and other hematologic effects, hindering its pharmaceutical applications. The nanoformulation was fabricated through the ultrasonication technique and optimized by selecting various parameters and concentrations for the formation of water-in-oil (*w/o*) emulsion. The optimized formulation depicts a smaller particle size of 213 nm with an encapsulation efficiency of approx. 80%. Further, nanoemulsion-based SSD lotion by utilizing argan oil as a cosmetotherapeutic agent was prepared for scar massaging with improved permeation properties. The designed cosmeceutical formulation was characterized in terms of physical appearance, refractive index, particle size, encapsulation efficiency, and biocompatibility. The compatibility of the formulation ingredients were determined through FTIR (Fourier Transform Infrared Spectroscopy). The formulated nanolotion containing SSD demonstrated superior antimicrobial activities against different bacterial strains in comparison to commercialized burn creams.

Keywords: nanolotion; silver sulphadiazine; cosmeceutical; antimicrobial therapy; argan oil

Citation: Fatima, Q.-u.a.; Ahmed, N.; Siddiqui, B.; Rehman, A.u.; Haq, I.u.; Khan, G.M.; Elaissari, A. Enhanced Antimicrobial Activity of Silver Sulfadiazine Cosmetotherapeutic Nanolotion for Burn Infections. *Cosmetics* **2022**, *9*, 93. https://doi.org/10.3390/cosmetics9050093

Academic Editor: Enzo Berardesca

Received: 3 August 2022
Accepted: 5 September 2022
Published: 9 September 2022

1. Introduction

Among different injuries and wounds, burns are one of the most debilitating, affecting almost every organ system, leading to significant causes of mortality. Infection of burn wounds, slow healing, hypertrophic scarring, and pain remain major challenges in the management of burn injuries [1,2]. This can be estimated from the fact that more than 50% of the mortality in burn patients is attributed to sepsis or other complications associated with burn wound infections. The burn injury occurs in response to tissue damage, arising from various factors. The most common factors include thermal, electrical, and radiation factors or any chemical contact, in which the thermal source varies from super-heated liquid, fire, hot metal, etc. [3]. Severe burn injuries lead to several bacterial infections due to creation of larger skin defects. The wound's infection progresses into severe sepsis accompanied by septicemia promoting further complications. Burn infections are considered as severe burn injuries that lead to several morbidities. The burn depth and area of the affected surface are also indicators of burn severity, while recent research indicates that a burn injury can become a chronic disease with the initiation of secondary pathologies [4]. Recent findings indicate that the population suffering from burn injuries produce sustained secondary conditions, such as homeostatic disruption, musculoskeletal disorders, anxiety, diabetes,

etc. [5]. The wounds of burns are mostly infected with bacterial species, e.g., *Escherichia coli*, *Staphylococcus aureus*, *Klebsiella*, and some of the fungal strains [6,7]. Microbial infection of the burnt surfaces causes slow healing and is responsible for 75% of mortality in patients having a burn surface of greater than 40% [8]. Most of the oral and parenteral antimicrobial formulations are not effective at preventing burn infection. For this purpose, a suitable topical antimicrobial agent is required, in addition to oral and parenteral antibiotic therapy for avoidance of serious complications [9,10].

Silver sulfadiazine (SSD) is the gold standard employed for the management of microbial infections in burn patients. It is approved by the Food and Drug administration, receiving widespread acceptance to control bacterial infections in second- and third-degree burns. It has a broad spectrum of activity against Gram-negative and Gram-positive bacteria, as well as possesses antifungal activities with low toxicity and good tolerability [11,12]. Currently available formulations of SSD possess various disadvantages, such as adhesive pseudo-eschar formation, which hinders the penetration of SSD and needs to be debrided for proper healing of burn wounds; a cream base, which further promotes inflammation and is deleterious to the healing of the wound bed; low solubility; and limited penetration [13–15]. Therefore, the need for a suitable formulation with targeted action at the burnt site is required [16]. Among the various techniques employed for overcoming these drawbacks, different types of nanocarriers provide the most logical solution with the provision of increased solubility and bioavailability to the formulation [17,18]. Nanoemulsions, also known as ultrafine emulsions, or nanosized submicron colloidal emulsions with droplet sizes under 500 nm, have attracted an immense amount of interest in research [19]. Owing to their high solubilization capacity, high surface area, low surfactant quantity, transparent or translucent appearance, simplicity of system, high kinetic stability, and easy-to-scale production, nanoemulsions are useful as a drug delivery system in the pharmaceutical field [19,20]. For potential pharmaceutical applications, both hydrophobic and hydrophilic drug molecules can be incorporated into the droplets of *o/w* or *w/o* nanoemulsions, by using high-energy or low-energy emulsification methods. Argan oil was introduced in the nanoemulsions as an external cosmeceutical agent, which possesses several important skin protective attributes, i.e., providing increased nutrients to the skin cells; stimulating intracellular oxygenation by neutralizing free radicals, thereby promoting re-epithelization; and possessing innate anti-inflammatory attributes [21]. In addition, argan oil also acts as a penetration enhancer in transdermal formulations [22].

After the patient survives from a burn, the complication of severe hypertrophic scarring arises, which further lengthens the process of normal healing by promoting the deposition of collagen at the burnt site with increased inflammation. These scars further pose erythema, pruritus, itching, pain, and limited mobility [23,24]. In this regard, massaging the scars with lotions and moisturizers is the mainstay therapy for the treatment of hypertrophic scars. Massaging through lotions helps to decrease the erythema, thickness of scars, and pain. These lotions also prevent the water loss from the transepidermis of skin.

This type of formulation not only provides protection to the skin but surpasses the pseudoeschar formed at the burn site, but also aids in decreasing the microbial infection [25,26]. The designed nanolotion enhances the skin permeation and allows for rapid active penetration through the skin, due to smaller particle size and larger surface area, thereby increasing the drug activity and being suitable for efficient delivery of active ingredients. It can penetrate through the rough skin surface while maintaining the feeling of the external phase. Surfactant-induced skin irritation is significantly reduced due to the addition of a limited amount of surfactant in nanoemulsions [27].

The ultimate goal of the current study was to design a method for the preparation of water-in-oil nanoemulsion-based cosmeceutical nanolotion to increase epithelization and wound healing with enhanced antimicrobial activity, i.e., antibacterial and antifungal activity of the drug. To the authors' knowledge, it is the first study that formulates an SSD-based nanolotion against antibacterial activity and for provision of massage therapy to burn patients.

2. Materials and Methods

2.1. Media, Chemicals, and Cell Lines

Cosmeceutical ingredient argan oil was purchased from Espace Cosmetics (Morocco). Silver sulfadiazine, ethanol, methanol, dimethyl sulfoxide (DMSO), tween-80, span-80, triton X-100, hydroxypropyl methyl cellulose phthalate (HPMCP), Methocel, cellulose acetate phthalate (CAP), and carbopol-934 were obtained from Sigma (Sigma-Aldrich Chemicals Germany). Ammonia was purchased from Scharlau Chemie (Barcelona, Spain). Nutrient agar media and potato dextrose agar from LabM Ltd. (Bury, UK). Nutrient broth from Qxoid Ltd. (Basingstoke, UK). Strains used for antibacterial assay include *Escherichia coli* (ATCC# 15224), *Klebsiella pneumoniae* (ATCC# 4617), and *Staphylococcus aureus* (ATCC# 6538). The fungal strain used was *Candida albicans* obtained from the fungal culture bank of Pakistan.

2.2. Formulation and Optimization of Blank Nanoemulsions

Water-in-oil nanoemulsions were prepared using ultrasonication method. Briefly, oil phase was prepared by addition of 5 mL of argan oil and emulsifier, which was stirred for 1 min at 100 rpm to ensure proper mixing. Separately, aqueous phase was prepared by taking 16% aqueous ammonia solution. The polymer was then added in an aqueous ammonia solution and stirred for 1 min at 100 rpm to ensure complete dissolution. The aqueous phase was then added to the oil phase dropwise under stirring conditions. The particle size of the internal droplets was further reduced by ultrasonication at 37 kHz ultrasound frequency using Elmasonic E 60 H ultrasonicator. Processed emulsions were collected for physical characterization. For optimization of blank nanoparticles, different emulsions were prepared by varying the polymers and surfactants with changing ratios and suitable surfactants were selected. In the second step, the formulation parameters such as stirring time, stirring rate, and ultrasonication time were optimized. The polymers employed in the formulation were hydroxypropyl methylcellulose phthalate (HPMCP), Methocel, and cellulose acetate phthalate (CAP), while span-80, triton X-100, and tween-80 were utilized as surfactants for formulation optimization.

2.3. Formulation and Optimization of Drug-Loaded Nanoemulsions

SSD-loaded nanoemulsion was prepared by weighing the desired amount of drug and adding it to 16% aqueous ammonia solution, in which polymer (HPMCP) was incorporated and stirred for the complete dissolution of drug. The aqueous phase was then added to the oil phase containing argan oil and span-80 dropwise under stirring conditions. The particle size was further reduced by ultrasonication at 37 kHz for 10 min to obtain SSD nanoemulsion.

2.4. Characterization and Evaluation of Nanoemulsions

2.4.1. Physical Appearance and Particle Size Analysis

The physical appearance of the resultant samples after ultrasonication was inspected visually for color, consistency, and phase separation. An emulsion without any phase separation, sedimentation, and creaming was considered acceptable. The droplet size of the most stable nanoemulsions was determined by using photon correlation spectroscopy (PCS), also known as dynamic light scattering (DLS) technique, which analyzes the fluctuations in laser light intensity that occur due to Brownian movement of the particles. The nanoemulsions (0.1 mL) were dispersed in 50 mL (500 times dilution) of distilled water in a volumetric flask and light scattering was monitored at 90° angle and 25 °C temperature.

2.4.2. Refractive Index Measurement

The refractive index of nanoemulsions (both blank and drug-encapsulated) was determined in triplicate using RFM 330 refractometer. Approximately 0.2 mL of the sample was placed on the surface of the prism to measure the refractive index at 25 °C.

2.4.3. Encapsulation Efficiency Measurement

The encapsulation efficiency of SSD-loaded nanoemulsions was taken as the percentage of SSD carried by the droplets and was determined in triplicate by using a UV-VIS double-beam spectrophotometer. For this purpose, free SSD molecules were determined by measuring the non-incorporated SSD present in the nanoemulsion after centrifugation using tabletop refrigerated centrifuge. For this purpose, SSD nanoemulsion was added to centrifugation tubes along with solvents, i.e., methanol and ammonia in 2:1 ratio, and centrifuged for 1 h at 13,000 rpm. After centrifugation, 2 mL supernatant was taken, which was then further diluted by using methanol and ammonia solution (2:1). The amount of SSD in supernatant was determined spectrophotometrically using UV-VIS double-beam spectrophotometer at λmax 254 nm. The SSD encapsulated in droplets was calculated from the difference between the total and the free SSD concentration [28].

$$\text{Encapsulation efficiency (\%)} = \text{Ct} - \text{Co/Ct} * 100 \quad (1)$$

where Co is the concentration of SSD detected in supernatant (free drug). Ct is the total concentration of SSD in the formulation.

2.5. Formulation of Nanolotion

The SSD-incorporated stable nanoemulsion was formulated into nanolotion. For this purpose, different concentrations of carbopol were taken in 2.5 mL of distilled water (50, 25, 12.5, and 6.25 mg) to make the nanolotion. When the carbopol was completely dissolved in water, this solution was added into the nanoemulsion to ensure complete dissolution. It was then stirred for about 3 min at 100 rpm using a magnetic stirrer to obtain nanolotion.

2.6. Characterization and Evaluation of Nanolotion

2.6.1. Physical Appearance and Particle Size Analysis

The physical appearance of the nanolotion was observed by visual inspection for its color, odor, and consistency. Particle size of the prepared nanolotion was determined using the same method as discussed in Section 2.4.1.

2.6.2. Fourier Transform Infrared Spectroscopy (FTIR)

The conformational stability of SSD was determined by (FTIR) Fourier transform infrared spectroscopy in the frequency range of 450–4000 cm^{-1} using a Perkin-Elmer spectrum 100 FTIR spectrometer. The FTIR spectra of blank, SSD-loaded nanoemulsion and nanolotion were obtained and compared to assess any changes occurring to SSD in form of nanoemulsions and nanolotion.

2.6.3. Comparative Antimicrobial Activity of Nanolotion

Antibacterial and antifungal activities of SSD-loaded nanolotion were compared with two commercially available creams—a local brand (Quench® (1% *w*/*w*) and a multinational cream (Dermazin® (1% *w*/*w*)—using the well diffusion method [29]. The bacterial strains used were *Escherichia coli*, *Klebsiella pneumoniae* (Gram-negative) and *Staphylococcus aureus* (Gram-positive), and *Candida albicans* was the fungal strain.

2.6.4. In Vivo Skin Irritation Assay (Biocompatibility Analysis)

In vivo skin irritation test was performed according to the previously reported method, with few modifications [30]. Rats were taken for performance of biocompatibility assay of the developed nanolotion and divided into three groups, each having 5 animals. First and second group were provided with a treatment of SSD-loaded nanolotion and 0.8% formalin, while the third group was taken as control group, without provision of any treatment. Scoring was given to each group based on developed erythema, irritation, and edema, in which '0–1' represent 'nonirritant', '2–3' present 'irritant', while '4–5' present 'strong irritant', after which the scoring given to each animal was added and 'primary

irritancy index (PII)' was calculated for each group. Irritation index of each group was also verified through histological analysis. For this purpose, after 24 h, sectioning of the skin samples was performed using cryostat microscope and analyzed under microscope. The characteristic structural analysis of the 'nanolotion'-treated skin was further investigated through FTIR. Molecular vibrations of the lipids present in the skin were analyzed over the range of 4000 cm^{-1} to 400 cm^{-1} [31].

2.6.5. Stability Studies

Stability studies for the developed nanolotion were performed at 4 ± 2 °C and 40 ± 2 °C with relative humidity of 75 ± 5 °C (accelerated stability studies) for a time period of 6 months. The study was performed according to ICH guidelines, by placing formulation in stability chamber for accelerated stability studies. The formulation was observed for its physical appearance, consistency, and particle size [22].

2.7. Statistical Analysis

The antimicrobial activity of nanolotion, Quench, and Dermazin cream was compared for all of the four strains (*Escherichia coli, Klebsiella pneumoniae, Staphylococcus aureus*, and *Candida albicans*) separately by applying one-way ANOVA (analysis of variance) and a post hoc test, i.e., LSD (least significant difference) using SPSS (Statistical Package for the Social Sciences).

3. Results and Discussions

3.1. Formulation and Optimization of Nanoemulsions

A high-energy ultrasonication method was used to prepare the blank emulsions. At first, the suitable polymer and surfactant with optimum quantities were selected by formulating various formulations, as depicted in Table 1. This set of experiments was performed by varying the type of polymer, surfactant, and their required quantities. HPMCP, CAP, and Methocel were used as the polymers; among these, increased sedimentation and phase separation were observed with Methocel. CAP, being insoluble in ammonia solution, was also omitted; while HPMCP, which brought out the most stable formulation, was selected for further optimization. After polymer selection, a suitable surfactant was selected by changing different surfactants in changing portions. Triton X-100, tween-80, and span-80 were tested for formulation optimization in different quantities, in which triton X-100 and tween-80 gave unstable formulations, both in single and combined forms, and led to phase separation upon ultrasonication, while the use of span 80 gave the most suitable formulation.

Table 1. Optimization of formulation based on polymers and surfactants.

Polymers/Surfactants	Concentrations	Response
Methocel (mg)	25	Sedimentation/phase separation
	50	Sedimentation/phase separation
CAP (mg)	25	Insolubility in ammonia solution
	50	Insolubility in ammonia solution
HPMCP (mg)	25	Stable emulsion
	50	Stable emulsion with larger particles
Tween80/span-80 (mL)	1	Phase separation upon ultrasonication
Methocel (mg)	25	Sedimentation/phase separation
Triton X100/span-80 (mL)	1	Phase separation upon ultrasonication
	2	Phase separation upon ultrasonication
TritonX100 (mL)	1	Unstable formulation
	2	Unstable formulation
Tween-80 (mL)	1	Unstable formulation
	2	Unstable formulation
Span-80 (mL)	1	Stable formulation (use less quantity)
	2	Stable formulation

In the second step, other process parameters such as ultrasonication time, stirring time, and stirring rate were optimized by changing these parameters through hit and trial, as shown in Table 2. Ultrasonication for 5 min produced larger particles of 400 nm, while ultrasonication for 10 min gave a particle size of 307.02 nm, whereas when the same emulsion was subjected to ultrasonication for 15 min, the particle size of the droplets came out to be 203 nm with high encapsulation efficiency. This is due to the increased residence time of the emulsion within the region of intense disruptive forces, which leads to the particle size reduction, while a further increase in ultrasonication time leads to an increase in particle size of 210 nm with lower encapsulation efficiency. This might be due to an increase in disruptive forces, which leads to lower encapsulation of drugs [32]. Similarly, increasing the stirring rate and stirring time decreased the particle size with lower encapsulation efficiency. The emulsion having an ultrasonication time of 15 min with a stirring rate of 20 rpm for 1 rpm was selected, as this emulsion was most stable when physical characterization was carried out and displayed no signs of sedimentation, creaming, coalescence, or phase inversion. The development of nanoemulsion formulation also depends on physicochemical properties of drugs. Aqueous ammonia solution was used to solubilize the SSD owing to the poor solubility of SSD in any other organic solvents and water. SSD is very slightly soluble in acetone and is practically insoluble in ethanol, diethyl ether, and chloroform, whereas it is freely soluble in ammonia solution [33].

Table 2. Optimization of formulation based on process parameters.

Process Parameters	Time	Response	
		Particle Size (nm)	EE (%)
Ultrasonication time	5	400	74
	10	307	78
	15	203	80.97
	20	210	75.5
Stirring rate (rpm)	10	240	
	20	203	
Stirring time (min)	1	203	
	2	215	

3.2. Characterization and Evaluation of Blank, Drug-Loaded Nanoemulsion and Nanolotion

3.2.1. Physical Characterization and Particle Size Analysis of Blank, Drug-Loaded Nanoemulsion and Nanolotion

The blank nanoemulsion appeared to be an off-white-colored viscous preparation, uniform in consistency, as depicted in Figure 1. Similarly, the SSD-incorporated nanoemulsion appeared to be uniform in consistency without any crystal formation, sedimentation, or creaming, whereas the nanolotion with 12.5 mg of carbopol 934-p was most stable and of desired consistency. The average diameters of the blank, SSD-loaded nanoemulsion and nanolotion measured by dynamic light-scattering technique came out to be nanometric in range, i.e., 170.02 nm, 203.83 nm, and 213.08 nm, respectively, as shown in Figure 1. The particle size of SSD loaded *w/o* nanoemulsion was slightly greater than the particle size of the blank emulsion due to incorporation of the drug, whereas the particle size of the nanolotion was greater than the SSD loaded *w/o* nanoemulsion; as carbopol was added to the nanoemulsion to form the nanolotion, some of the carbopol may stick to the surface of the particles, which might be a reason for the slight increase in the particle size of the nanolotion.

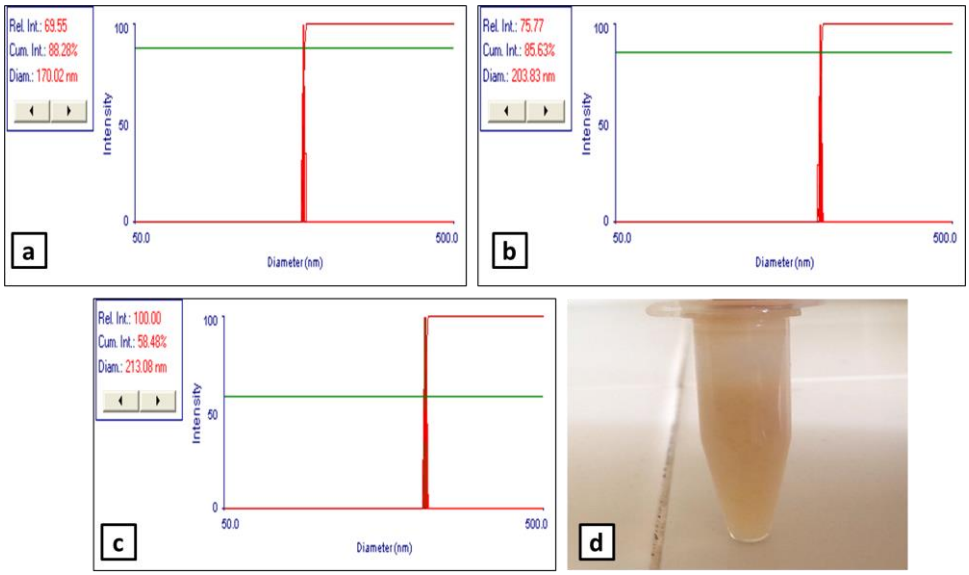

Figure 1. (**a**) Particle size of blank formulation, (**b**) SSD-loaded formulation, and (**c**) SSD-loaded nanolotion; and (**d**) appearance of SSD-nanolotion. The red peak is basically presenting the size.

3.2.2. Refractive Index Measurement

The refractive indexes of the nanoemulsions (both blank and drug-encapsulated) were determined in triplicate using an RFM 330 refractometer. The refractive indexes of the blank and drug-loaded nanoemulsion were measured in triplicate. The refractive indexes of the blank nanoemulsion and SSD-loaded nanoemulsion were 1.341 and 1.349, respectively, without any significant difference (p-value > 0.05), which indicates that the SSD-loaded nanoemulsion was not only physically stable but also chemically stable and remained isotropic in nature; thus, no interaction occurred between the SSD and excipients present in the nanoemulsion.

3.2.3. Encapsulation Efficiency Measurement

The encapsulation efficiencies of the SSD-loaded nanoemulsion and nanolotion were determined in triplicate using UV-VIS spectrophotometer. The SSD nanoemulsion and nanolotion were centrifuged in the presence of two solvents, i.e., methanol and 1% ammonia, in 2:1 ratio due to the poor solubility of SSD in organic solvents and water [34]. The encapsulation efficiency of the SSD-loaded nanoemulsion was 80.97%, whereas the encapsulation efficiency of the nanolotion was 80.87%.

3.2.4. Fourier Transform Infrared Spectroscopy

Infrared spectra represent the fingerprint of the sample by measuring the absorption of infrared radiations by the sample material versus the wavelength. To check the possible interactions between the drug and excipients, the spectra for blank nanoemulsion, SSD-loaded nanoemulsion, and nanolotion were obtained directly using a Perkin Elmer FTIR spectrometer, as shown in Figure 2. FTIR measures the absorption of IR radiation by the sample material versus the wavelength due to the vibration of specific chemical bonds in the sample. The observation of the vibration spectrum of blank emulsion, SSD-loaded nanoemulsion, and nanolotion allows for the evaluation of any kind of interaction occurring between the drug and the excipients, as the vibration of atoms due to interactions may alter the frequencies of absorption. The infrared assignment of different functional groups is shown in Table 3. The FTIR spectra of SSD-loaded nanoemulsion and nanolotion showed prominent peaks in the regions of 1165 and 1240.77 cm^{-1}, respectively, due to S=O asymmetry; the functional group was present only in SSD, whereas the peak in this region was absent in blank emulsion spectra. Peaks present in the spectra of blank emulsion can be seen in the spectra of the SSD-loaded nanoemulsion and nanolotion [35]. Overall spectra

for all three formulations and the range of peaks remained unchanged, which indicates a lack of interaction in any of the formulations. In a study of FTIR spectra of a gel containing SSD and HPMC compared with pure drug (SSD), the major peaks observed were for the functional groups C-H, N-H and S=O at 2982, 3333, and 1040 cm^{-1}, respectively [36], which is almost similar to results of the present study, i.e., 3009.63, 3434, and 1240.77 cm^{-1} for C-H, N-H, and S=O, respectively, in the case of the nanolotion; whereas in the case of the SSD-loaded nanoemulsion, these values were 2923.95, 3435.70, and 1165.70 cm^{-1}, respectively [37].

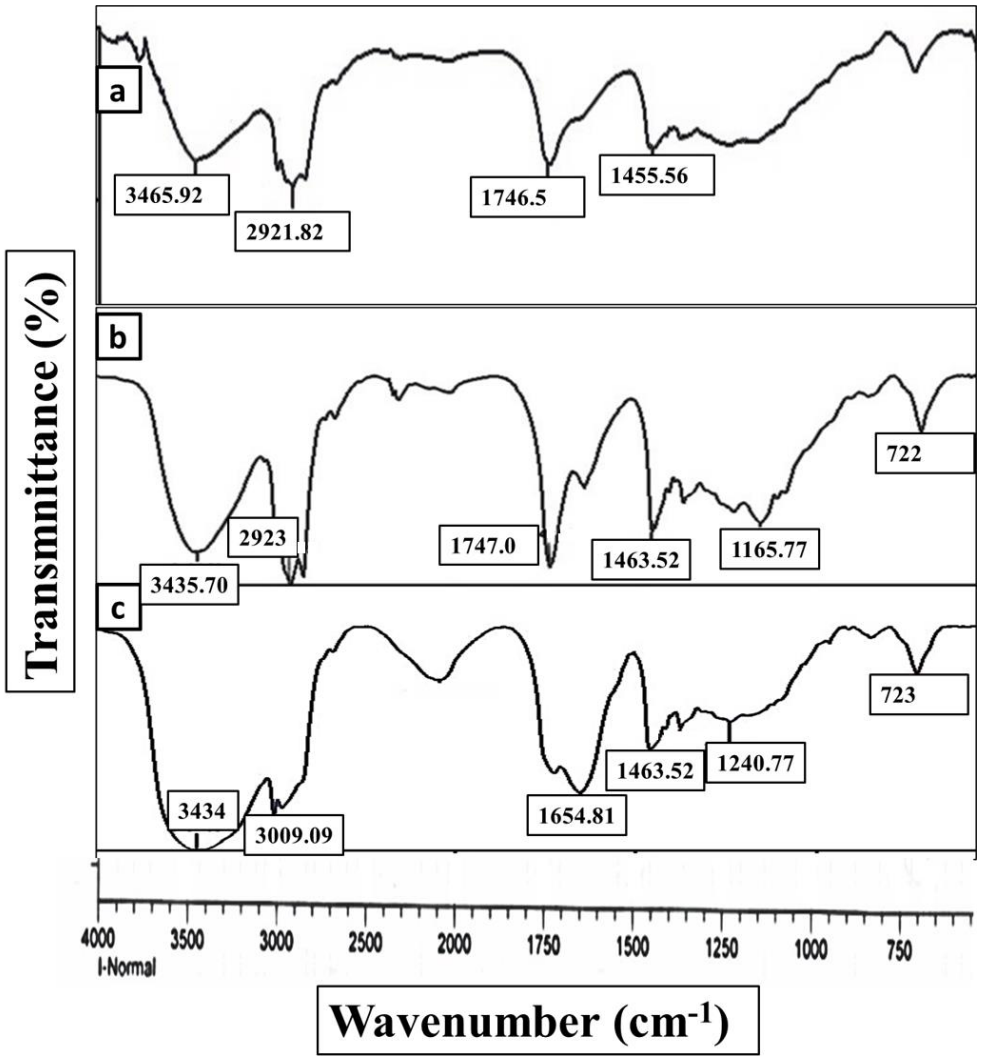

Figure 2. (**a**) FTIR spectra of blank formulation; (**b**) SSD-loaded formulation; (**c**) SSD-loaded nanolotion.

Table 3. Interpretation of FT-IR spectra of blank, SSD-loaded nanoemulsion, and nanolotion.

Functional Groups	Blank Nanoemulsions	SSD Loaded Nanoemulsion
N-H stretch	3465.92	3435.70
C-H stretch	2921.82	2923.95
C=O stretch	1746.58	1747.00
S=O	-	1165.77
Fingerprint region	1455.56	1463.52

3.2.5. Comparative In Vitro Antibacterial Study

The antibacterial activity of the nanolotion was compared with two commercialized creams using two Gram-negative and a Gram-positive bacterial strain, as depicted in

Figure 3. The marketed creams were 'Quench' cream (local brand) and 'Dermazin', a multinational cream, in order to determine whether the antibacterial activity is comparable to commercialized creams. For that purpose, a statistical comparison was carried out by applying ANOVA and LSD. The one-way ANOVA is used to determine whether there are any significant differences between the means of three or more independent (unrelated) groups. The result of the test showed *p*-values of 0.001, 0.018, and 0.280 for *E. coli*, *K. pneumoniae*, and *S. aureus*, respectively. The results of the one-way ANOVA indicate the overall difference between the groups (the *p*-value obtained for the Gram-negative strain); *E. coli* was 0.001, which indicates that a significant difference exists in the antimicrobial activity of the three formulations (i.e., nanolotion, Quench, and Dermazin), whereas the *p*-value obtained for *K. pneumoniae* (the Gram-negative strain) was 0.018, which indicates a significant difference in the antibacterial activity of three formulations. However, the *p*-value for the Gram-positive strain *S. aureus* came out to be 0.280, which indicates that no significant differences exist between the antibacterial activity of the three formulations, i.e., they have comparable antibacterial activity against the *S. aureus*. One-way ANOVA is an omnibus test statistic and cannot tell which specific groups were significantly different from each other (whether it is nanolotion and Quench, nanolotion and Dermazin, or Quench and Dermazin). To determine which specific groups differed from each other, post hoc test LSD was applied using SPSS, in which pairwise comparison of groups was carried out. Post hoc test LSD was then applied; in the case of *E. coli*, the *p*-value obtained for nanolotion and Quench was 0.018, for nanolotion and Dermazin it was 0.001, and for Quench and Dermazin the *p*-value came out to be 0.006, which indicates significant differences between nanolotion and Quench, nanolotion and Dermazin, and Quench and Dermazin, respectively. ZOI values as well as *p*-values indicate that the nanolotion has a superior antibacterial activity against *E. coli* as compared to the commercialized creams, i.e., Quench and Dermazin.

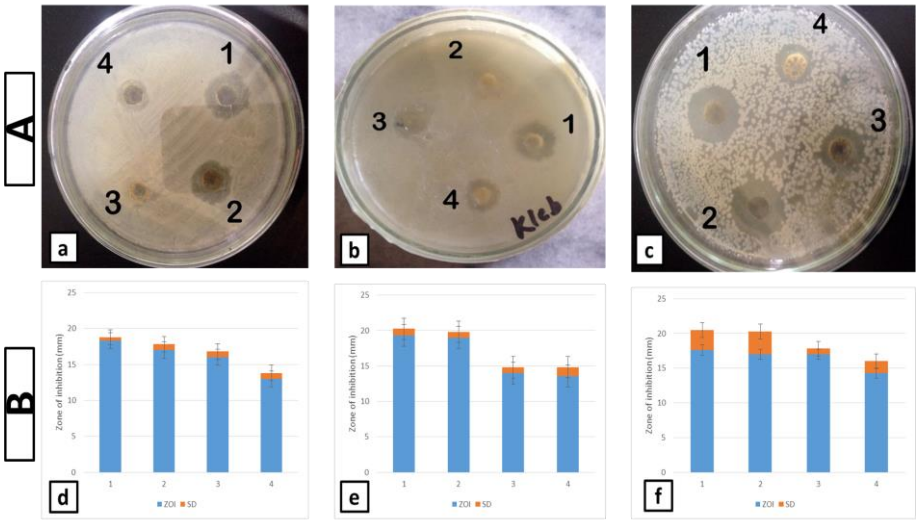

Figure 3. (**A**). In vitro antibacterial comparison of (1) nanolotion in DMSO, (2) nanolotion in water, (3) Quench cream, and (4) Dermazin cream of, (**a**) *E. coli*, (**b**) *K. pneumoniae*, and (**c**) *S. aureus*. (**B**). Comparison of In vitro anti-bacterial ZOI (mm) of (1) nanolotion in DMSO (2) nanolotion in water (3) Quench cream (4) Dermazin cream of, (**d**) *E. coli*, (**e**) *K. pneumoniae*, and (**f**) *S. aureus*.

The *p*-values obtained for nanolotion and Quench, nanolotion and Dermazin, and Quench and Dermazin were 0.104, 0.004, and 0.005, respectively, when *K. pneumoniae* was used as a bacterial strain. These values showed that no significant differences exist between the nanolotion and Quench, and a significant difference exists between the nanolotion and Dermazin and Quench and Dermazin. Thus, it can be concluded that nanolotion and Quench have a comparable antibacterial activity against *K. pneumoniae*, and this antibacterial activity is superior to Dermazin. When the Gram-positive strain *S. aureus* is

used, the *p*-values obtained for nanolotion and Quench, nanolotion and Dermazin, and Quench and Dermazin were 0.748, 0.143, and 0.227, respectively. These values indicate that no significant differences exist in the antibacterial activity of the three formulations (i.e., nanolotion, Quench, and Dermazin), and they have the similar antibacterial activity against the Gram-positive strain *S. aureus*.

3.2.6. In Vitro Antifungal Study

Candida albicans was used to compare the antifungal activity of the nanolotion with two commercialized creams. In case of the antifungal strain *C. albicans*, the *p*-value obtained was 0.014, which specifies a significant difference in the antifungal activity of three formulations, as shown in Figure 4. Post hoc test LSD was then applied, in which the *p*-values obtained for the antifungal strain *C albicans* were 0.007, 0.016, and 0.488 for nanolotion and Quench, nanolotion and Dermazin, and Quench and Dermazin, respectively. The first two values suggest that significant differences exist between the nanolotion and Quench and the nanolotion and Dermazin, i.e., the antifungal activity of the nanolotion is greater compared to the commercialized creams Quench and Dermazin, whereas the third value suggests no significant difference in the antifungal activity of Quench and Dermazin, i.e., both the commercialized creams have comparable antifungal activity.

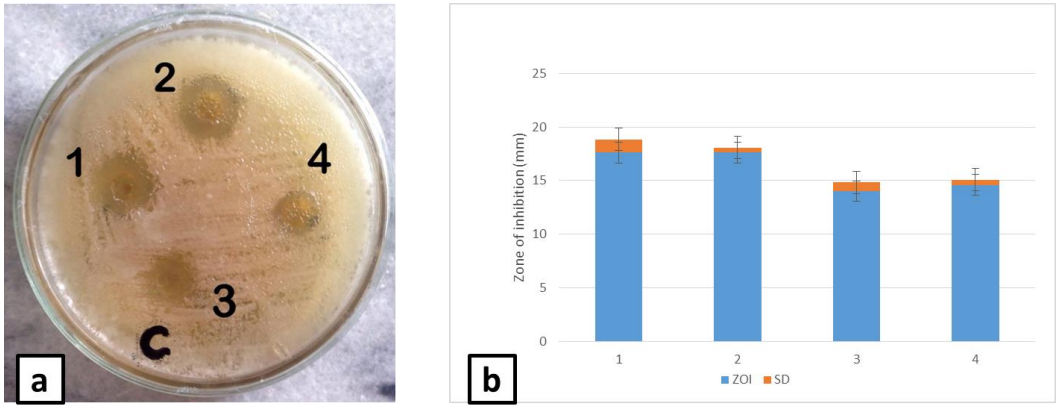

Figure 4. (**a**) Antifungal assay and (**b**) in vitro antifungal comparison of (1) nanolotion in DMSO, (2) nanolotion in water, (3) Quench cream, and (4) Dermazin cream.

3.2.7. In Vivo Skin Irritation Assay (Biocompatibility Analysis)

In vivo skin irritation assay or biocompatibility studies demonstrated negative reactions to any erythema and edema with the control and SSD-loaded nanolotion-treated skin. The primary irritancy index (PII) was calculated for control group, 0.8 % formalin, and SSD-loaded nanolotion as shown in Table 4. PII obtained for the control and SSD-loaded nanolotion-treated skin was 0 and 0.66, respectively, illustrating that no significant difference was observed between the two groups ($p < 0.05$). However, the PII obtained for 0.8% formalin was 4, indicating a severe irritation index. In addition, histological analysis further confirmed the safety profile of the SSD-loaded nanolotion, as depicted in Figure 5a. The developed nanolotion-treated skin displayed a similar histological profile as that of untreated skin, except for the appearance of slight edema due to the retention of formulation in the skin layers. However, pronounced epidermal skin damage and severe edema were produced with that of standard irritant solution. The results produced from FTIR studies displayed minute differences in the molecular vibrations of the two groups. The most prominent peaks at 2923 cm^{-1} and 2852 cm^{-1} represent the hydrocarbon chains of the lipids. Moreover, bands at 1551 and 1634 cm^{-1} arose due to amide vibrations of stratum corneum. The molecular vibration obtained at 1743 cm^{-1} represents the presence of the ester band. These observations illustrate the safety profile of the developed nanolotion.

Table 4. Comparative primary irritancy index (PII) of SSD-loaded nanolotion.

Time (h)	Control		Formalin (0.8%)		SSD-Loaded Nanolotion	
	Erythema	Edema	Erythema	Edema	Erythema	Edema
0	0	0	0	0	0	0
6	0	0	2	3	0	1
24	0	0	4	3	0	1
Mean ± SD	0 ± 0	0 ± 0	2 ± 2	2 ± 1.7	0 ± 0	0.66 ± 0.5
PII	0		4		0.66	

Where PII = primary irritancy index.

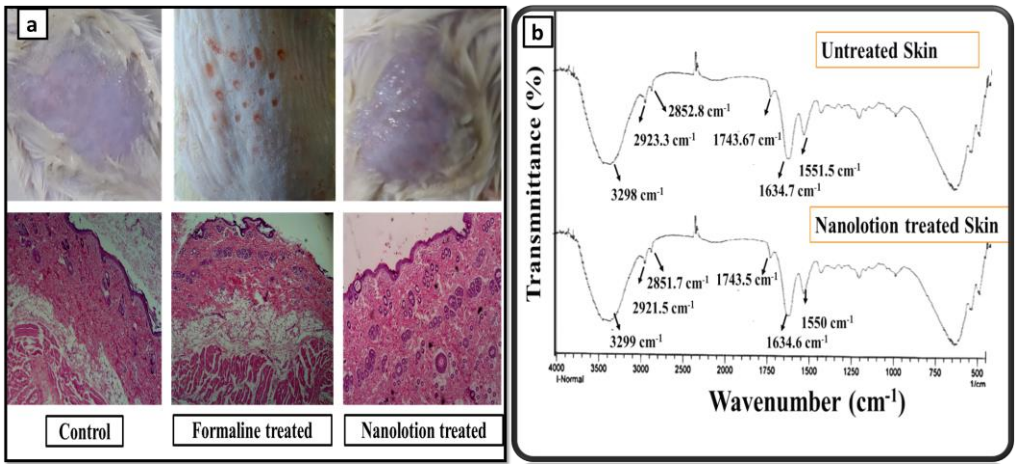

Figure 5. Biocompatibility studies of SSD nanolotion. (**a**) Skin irritation and histological analysis under microscope; (**b**) FTIR spectra of SSD nanolotion and formalin-treated skin.

Stability Studies

The developed nanolotion displayed no significant change in its physical appearance and particle size during the stability studies performed for 6 months. The results are illustrated in Table 5, indicating the long-term stability of the nanolotion.

Table 5. Stability studies for SSD-based nanolotion.

Temperature (±2 °C)	Physical Appearance			Mean Particle Size		
	1 Month	3 Month	6 Month	1 Month	3 Month	6 Month
4	Physically stable	Physically stable	Physically stable	213 nm	215 nm	218 nm
40	Physically stable	Physically stable	Physically stable, slight phase separation	213 nm	217 nm	225 nm

4. Conclusions

SSD was incorporated into the designated nanoemulsion systems and was eventually formulated into nanolotion with good encapsulation efficiency. The particle size of the optimized formulation was in the nanometric range. The refractive index and FTIR spectra of the blank, drug-loaded nanoemulsion and nanolotion suggest that the formulation was stable, and no chemical interaction occurred between the drug and excipients. Formulating the SSD nanoemulsion into the nanolotion using the cosmeceutical agent 'argan oil' demonstrated enhanced antibacterial and antifungal activity (in Gram-negative and fungal strain cases) due to the extremely large surface area of the nanocarriers in comparison to the marketed creams. Moreover, biocompatibility studies for the developed lotion also proved its efficacy, without any irritation index. In short, the prepared SSD-incorporated

nanolotion can be an ideal carrier for delivering the therapeutic agent with the provision of enhanced nourishment and protection to the skin due to presence of argan oil, thus promoting rapid and complete epithelization and healing of burn wounds, leading the way towards a strong cosmetotherapeutic formulation.

Author Contributions: Conceptualization, Q.-u.a.F. and N.A.; methodology, Q.-u.a.F. and A.u.R.; validation, B.S., G.M.K. and N.A.; formal analysis, B.S., I.u.H. and A.u.R.; writing—original draft preparation, Q.-u.a.F. and B.S.; writing—review and editing, B.S., A.u.R., I.u.H. and A.E.; supervision, G.M.K. and N.A.; project administration, G.M.K., A.E. and I.u.H.; funding acquisition, A.E. All authors have read and agreed to the published version of the manuscript.

Funding: This research received no external funding.

Institutional Review Board Statement: Not applicable.

Informed Consent Statement: Not applicable.

Data Availability Statement: The data presented in this study are available in article.

Conflicts of Interest: The authors declare no conflict of interest.

References

1. Souto, E.B.; Ribeiro, A.F.; Ferreira, M.I.; Teixeira, M.C.; Shimojo, A.A.; Soriano, J.L.; Naveros, B.C.; Durazzo, A.; Lucarini, M.; Souto, S.B. New nanotechnologies for the treatment and repair of skin burns infections. *Int. J. Mol. Sci.* **2020**, *21*, 393. [CrossRef] [PubMed]
2. Koyro, K.I.; Bingoel, A.S.; Bucher, F.; Vogt, P.M. Burn Guidelines—An International Comparison. *Eur. Burn. J.* **2021**, *2*, 125–139. [CrossRef]
3. Hu, X.; Sun, Z.; Li, F.; Jiang, C.; Yan, W.; Sun, Y. Burn-induced heterotopic ossification from incidence to therapy: Key signaling pathways underlying ectopic bone formation. *Cell. Mol. Biol. Lett.* **2021**, *26*, 1–13. [CrossRef] [PubMed]
4. Oba, J.; Okabe, M.; Yoshida, T.; Soko, C.; Fathy, M.; Amano, K.; Kobashi, D.; Wakasugi, M.; Okudera, H. Hyperdry human amniotic membrane application as a wound dressing for a full-thickness skin excision after a third-degree burn injury. *Burn. Trauma* **2020**, *8*, tkaa014. [CrossRef]
5. Barrett, L.W.; Fear, V.S.; Waithman, J.C.; Wood, F.M.; Fear, M.W. Understanding acute burn injury as a chronic disease. *Burn. Trauma* **2019**, *7*, s41038-019-0163-2. [CrossRef]
6. Shao, W.; Liu, H.; Liu, X.; Wang, S.; Wu, J.; Zhang, R.; Min, H.; Huang, M. Development of silver sulfadiazine loaded bacterial cellulose/sodium alginate composite films with enhanced antibacterial property. *Carbohydr. Polym.* **2015**, *132*, 351–358. [CrossRef]
7. de Sousa, J.K.T.; Haddad, J.P.A.; de Oliveira, A.C.; Vieira, C.D.; dos Santos, S.G. In vitro activity of antimicrobial-impregnated catheters against biofilms formed by KPC-producing Klebsiella pneumoniae. *J. Appl. Microbiol.* **2019**, *127*, 1018–1027. [CrossRef] [PubMed]
8. Klifto, K.M.; Gurno, C.F.; Seal, S.M.; Hultman, C.S. Factors associated with mortality following burns complicated by necrotizing skin and soft tissue infections: A systematic review and meta-analysis of individual participant data. *J. Burn. Care Res.* **2021**, *43*, 163–188. [CrossRef]
9. Nuutila, K.; Grolman, J.; Yang, L.; Broomhead, M.; Lipsitz, S.; Onderdonk, A.; Mooney, D.; Eriksson, E. Immediate treatment of burn wounds with high concentrations of topical antibiotics in an alginate hydrogel using a platform wound device. *Adv. Wound Care* **2020**, *9*, 48–60. [CrossRef]
10. Bocchiotti, G.; Robotti, E. The use of a topical antibacterial agent (silver sulfadiazine) on soft-tissue wounds. *Minerva Chir.* **1990**, *45*, 677–681.
11. Khattak, S.; Qin, X.-T.; Huang, L.-H.; Xie, Y.-Y.; Jia, S.-R.; Zhong, C. Preparation and characterization of antibacterial bacterial cellulose/chitosan hydrogels impregnated with silver sulfadiazine. *Int. J. Biol. Macromol.* **2021**, *189*, 483–493. [CrossRef]
12. Heyneman, A.; Hoeksema, H.; Vandekerckhove, D.; Pirayesh, A.; Monstrey, S. The role of silver sulphadiazine in the conservative treatment of partial thickness burn wounds: A systematic review. *Burns* **2016**, *42*, 1377–1386. [CrossRef]
13. Luan, J.; Wu, J.; Zheng, Y.; Song, W.; Wang, G.; Guo, J.; Ding, X. Impregnation of silver sulfadiazine into bacterial cellulose for antimicrobial and biocompatible wound dressing. *Biomed. Mater.* **2012**, *7*, 065006. [CrossRef]
14. Oaks, R.J.; Cindass, R. *Silver Sulfadiazine*; StatPearls: Treasure Island, FL, USA, 2021.
15. El-Feky, G.S.; Sharaf, S.S.; El Shafei, A.; Hegazy, A.A. Using chitosan nanoparticles as drug carriers for the development of a silver sulfadiazine wound dressing. *Carbohydr. Polym.* **2017**, *158*, 11–19. [CrossRef]
16. Irshad, S.; Siddiqui, B.; ur Rehman, A.; Farooq, R.K.; Ahmed, N. Recent trends and development in targeted delivery of therapeutics through enzyme responsive intelligent nanoplatform. *Int. J. Polym. Mater. Polym. Biomater.* **2022**, *71*, 403–413. [CrossRef]

17. Jahromi, M.A.M.; Zangabad, P.S.; Basri, S.M.M.; Zangabad, K.S.; Ghamarypour, A.; Aref, A.R.; Karimi, M.; Hamblin, M.R. Nanomedicine and advanced technologies for burns: Preventing infection and facilitating wound healing. *Adv. Drug Deliv. Rev.* **2018**, *123*, 33–64. [CrossRef] [PubMed]
18. Siddiqui, B.; Al-Dossary, A.A.; Elaissari, A.; Ahmed, N. Exploiting recent trends for the synthesis and surface functionalization of mesoporous silica nanoparticles towards biomedical applications. *Int. J. Pharm. X* **2022**, *4*, 100116. [CrossRef] [PubMed]
19. Chime, S.; Kenechukwu, F.; Attama, A. Nanoemulsions—Advances in formulation, characterization and applications in drug delivery. In *Application of Nanotechnology in Drug Delivery*; BoD–Books on Demand: Norderstedt, Germany, 2014; Volume 3.
20. Naseema, A.; Kovooru, L.; Behera, A.K.; Kumar, K.P.; Srivastava, P. A critical review of synthesis procedures, applications and future potential of nanoemulsions. *Adv. Colloid Interface Sci.* **2020**, *287*, 102318.
21. Menni, H.B.; Belarbi, M.; Menni, D.B.; Bendiab, H.; Kherraf, Y.; Ksouri, R.; Djebli, N.; Visioli, F. Anti-inflammatory activity of argan oil and its minor components. *Int. J. Food Sci. Nutr.* **2020**, *71*, 307–314. [CrossRef]
22. Siddiqui, B.; Rehman, A.U.; Haq, I.-U.; Ahmad, N.M.; Ahmed, N. Development, optimisation, and evaluation of nanoencapsulated diacerein emulgel for potential use in osteoarthritis. *J. Microencapsul.* **2020**, *37*, 595–608. [CrossRef]
23. Čoma, M.; Fröhlichová, L.; Urban, L.; Zajíček, R.; Urban, T.; Szabo, P.; Novák, Š.; Fetissov, V.; Dvořánková, B.; Smetana, K. Molecular changes underlying hypertrophic scarring following burns involve specific deregulations at all wound healing stages (Inflammation, proliferation and maturation). *Int. J. Mol. Sci.* **2021**, *22*, 897. [CrossRef] [PubMed]
24. Shu, F.; Liu, H.; Lou, X.; Zhou, Z.; Zhao, Z.; Liu, Y.; Bai, X.; Luo, P.; Zheng, Y.; Xiao, S. Analysis of the excellent predictors of postburn hypertrophic scarring pain and neuropathic pain. *Burns* **2021**, *48*, 1425–1434. [CrossRef] [PubMed]
25. Field, T.; Peck, M.; Hernandez-Reif, M.; Krugman, S.; Burman, I.; Ozment-Schenck, L. Postburn itching, pain, and psychological symptoms are reduced with massage therapy. *J. Burn. Care Rehabil.* **2000**, *21*, 189–193. [CrossRef]
26. Vinaik, R.; Fish, J.; Jeschke, M.G. Burn Hypertrophic Scar in Pediatric Patients: Clinical Case. In *Textbook on Scar Management*; Springer: Berlin/Heidelberg, Germany, 2020; pp. 517–521.
27. Nithianandam, P.; Das, S.; Park, Y.C. Effect of Surfactant–Keratin Hydrolysate Interactions on the Hydration Properties of a Stratum Corneum Substitute. *Langmuir* **2020**, *36*, 2543–2552. [CrossRef] [PubMed]
28. Ragavan, M.L.; Das, N. Nanoencapsulation of Saccharomycopsis fibuligera VIT-MN04 using electrospinning technique for easy gastrointestinal transit. *IET Nanobiotechnol.* **2020**, *14*, 766–773. [CrossRef] [PubMed]
29. Bhatia, D.; Mittal, A.; Malik, D.K. Antimicrobial potential and in vitro cytotoxicity study of polyvinyl pyrollidone-stabilised silver nanoparticles synthesised from Lysinibacillus boronitolerans. *IET Nanobiotechnol.* **2021**, *15*, 427–440. [CrossRef]
30. Draize, J.H.J. Methods for the study of irritation and toxicity of substances applied topically to the skin and mucous membranes. *J. Pharmacol. Exp. Ther.* **1944**, *82*, 377–390.
31. Dar, M.J.; Din, F.U.; Khan, G.M. Sodium stibogluconate loaded nano-deformable liposomes for topical treatment of leishmaniasis: Macrophage as a target cell. *J. Drug Deliv.* **2018**, *25*, 1595–1606. [CrossRef]
32. Mahbubul, I.; Elcioglu, E.B.; Saidur, R.; Amalina, M. Optimization of ultrasonication period for better dispersion and stability of TiO_2—water nanofluid. *Ultrason. Sonochem.* **2017**, *37*, 360–367. [CrossRef]
33. Venkataraman, M.; Nagarsenker, M.J.A.P. Silver sulfadiazine nanosystems for burn therapy. *AAPS PharmSciTech* **2013**, *14*, 254–264. [CrossRef]
34. Morsi, N.M.; Abdelbary, G.A.; Ahmed, M.A. Silver sulfadiazine based cubosome hydrogels for topical treatment of burns: Development and in vitro/in vivo characterization. *Eur. J. Pharm. Biopharm.* **2014**, *86*, 178–189. [CrossRef] [PubMed]
35. Felciya, S.J.G.; Devi, M.V.; Ramanathan, G.; Poornima, V.; Sivagnanam, U.T. Fabrication of polyhydroxy butyric acid–Gelatin blended nanofibrous matrix integrated with silver sulfadiazine as an alternate wound dressing for treating burns. *Mater. Lett.* **2021**, *282*, 128541. [CrossRef]
36. Mehta, P.; Sharma, D.; Dashora, A.; Sahu, D.; Garg, R.; Agrawal, P.; Kapoor, D. Design, development and evaluation of lipid based topical formulations of silver sulfadiazine for treatment of burns and wounds. *Innovare J. Life Sci.* **2013**, *1*, 38–44.
37. Khattak, S.; Qin, X.-T.; Wahid, F.; Huang, L.-H.; Xie, Y.-Y.; Jia, S.-R.; Zhong, C. Permeation of Silver Sulfadiazine Into TEMPO-Oxidized Bacterial Cellulose as an Antibacterial Agent. *Front. Bioeng. Biotechnol. Adv.* **2020**, *8*, 616467. [CrossRef] [PubMed]